Beamspace Adaptive Beamforming for Hydrodynamic Towed Array Self-Noise Cancellation

*Vincent E. Premus, Stephen M. Kogon, and James Ward**
MIT Lincoln Laboratory
244 Wood Street, Lexington, MA 02420
vpremus@ll.mit.edu

ABSTRACT

A beamspace adaptive beamformer implementation for the rejection of cable strum self-noise on passive sonar towed arrays is presented. The approach focuses on the implementation of a white noise gain constraint based on the scaled projection technique due to Cox et al. [IEEE Trans. on ASSP, Vol. 35 (10), Oct. 1987]. The objective is to balance the aggressive adaptation necessary for nulling the strong mainlobe interference represented by cable strum against the conservative adaptation required for protection against signal self-nulling associated with steering vector mismatch. Particular attention is paid to the definition of white noise gain as the metric that reflects the level of mainlobe adaptive nulling for an adaptive beamformer. Adaptation control is subsequently performed through the implementation of a constraint on maximum allowable white noise gain at the output of the adaptive processor. The theoretical development underlying the scaled projection based constraint implementation is reviewed. Towed array data results depicting the performance gain of the new ABF algorithm optimized for strum cancellation relative to that of a more conservative baseline ABF algorithm are presented.

1. INTRODUCTION

Hydrodynamic self-noise on passive sonar towed arrays has been a well-known performance-limiting factor for ocean acoustic source detection at low frequency [1]. High wavenumber mechanical vibrations are induced in the array by vortex shedding associated with hydrodynamic flow over the array body and cable scope. These vibrations are know to couple into the hydrophone array as coherent acoustic noise sources and can impair acoustic detection performance, particularly in the forward endfire direction. As a direct consequence of its spatially coherent nature, it has been shown that cable strum noise effects can be mitigated via adaptive processing [2]. In this work, a new approach to coherent strum noise mitigation, based on a beamspace adaptive beamformer (ABF) architecture with a white noise gain constraint (WNGC) that emphasizes mainlobe interference nulling is introduced. Finally, data results illustrating the performance improvement over an existing beamspace ABF algorithm that emphasizes robustness to mismatch-induced self-nulling are presented.

2. THE PHYSICS OF CABLE STRUM

2.1 Vortex shedding

When an array is subject to hydrodynamic flow with a component normal to its axis, a wake is formed. When the velocity of the transverse flow increases beyond a certain threshold, eddies, or vortices, begin to form and separate from the wake. Eventually these vortices shed from the wake in an asymmetric fashion [3]. This asymmetric shedding imparts an oscillatory lift force locally on the array which, depending on the properties of the array such as tension and density, can excite transverse vibrations which propagate along the array axis. The frequency of vortex shedding in hydrodynamic flow is related to properties of the flow and the array via the empirically determined Strouhal relation [1]:

$$f_s = \frac{Sv}{d},$$

where S is the Strouhal number, equal to 0.21 in the laminar flow regime characteristic of most towed array environments, v is the velocity of flow normal to the array axis, and d is the cable diameter. Note that the normal component of velocity of flow can vary with time in response to platform motion and local inhomogeneities in the turbulent medium.

The transfer function to which the Strouhal excitation is applied is governed by the wave equation subject to the boundary conditions of the array under tow. For example, assuming fixed boundary conditions for the array, the preferred frequencies of vibration or modes of the array

Sponsored in part by PEO-USW ASTO, under Air Force Contract F19628-00-C-0002. Opinions, interpretations, conclusions, and recommendations are those of the author and are not necessarily endorsed by the U.S. Air Force.

Report Documentation Page

Form Approved
OMB No. 0704-0188

Public reporting burden for the collection of information is estimated to average 1 hour per response, including the time for reviewing instructions, searching existing data sources, gathering and maintaining the data needed, and completing and reviewing the collection of information. Send comments regarding this burden estimate or any other aspect of this collection of information, including suggestions for reducing this burden, to Washington Headquarters Services, Directorate for Information Operations and Reports, 1215 Jefferson Davis Highway, Suite 1204, Arlington VA 22202-4302. Respondents should be aware that notwithstanding any other provision of law, no person shall be subject to a penalty for failing to comply with a collection of information if it does not display a currently valid OMB control number.

1. REPORT DATE	2. REPORT TYPE	3. DATES COVERED
14 MAR 2001	**N/A**	**-**

4. TITLE AND SUBTITLE
Beamspace Adaptive Beamforming for Hydrodynamic Towed Array Self-Noise Cancellation

5a. CONTRACT NUMBER
F19628-00-C-0002

5b. GRANT NUMBER

5c. PROGRAM ELEMENT NUMBER

6. AUTHOR(S)
Vincent E. Premus; Stephen M. Kogon; James Ward

5d. PROJECT NUMBER

5e. TASK NUMBER

5f. WORK UNIT NUMBER

7. PERFORMING ORGANIZATION NAME(S) AND ADDRESS(ES)
MIT Lincoln Laboratory 244 Wood Street, Lexington, MA 02420

8. PERFORMING ORGANIZATION REPORT NUMBER

9. SPONSORING/MONITORING AGENCY NAME(S) AND ADDRESS(ES)

10. SPONSOR/MONITOR'S ACRONYM(S)

11. SPONSOR/MONITOR'S REPORT NUMBER(S)

12. DISTRIBUTION/AVAILABILITY STATEMENT
Approved for public release, distribution unlimited

13. SUPPLEMENTARY NOTES
See ADM001263 for entire Adaptive Sensor Array Processing Workshop.

14. ABSTRACT
.A beamspace adaptive beamformer implementation for the rejection of cable strum self-noise on passive sonar towed arrays is presented. The approach focuses on the implementation of a white noise gain constraint based on the scaled projection technique due to Cox et al. [IEEE Trans. on ASSP, Vol. 35 (10), Oct. 1987]. The objective is to balance the aggressive adaptation necessary for nulling the strong mainlobe interference represented by cable strum against the conservative adaptation required for protection against signal selfnulling associated with steering vector mismatch. Particular attention is paid to the definition of white noise gain as the metric that reflects the level of mainlobe adaptive nulling for an adaptive beamformer. Adaptation control is subsequently performed through the implementation of a constraint on maximum allowable white noise gain at the output of the adaptive processor. The theoretical development underlying the scaled projection based constraint implementation is reviewed. Towed array data results depicting the performance gain of the new ABF algorithm optimized for strum cancellation relative to that of a more conservative baseline ABF algorithm are presented.

15. SUBJECT TERMS

16. SECURITY CLASSIFICATION OF:			17. LIMITATION OF ABSTRACT	18. NUMBER OF PAGES	19a. NAME OF RESPONSIBLE PERSON
a. REPORT	b. ABSTRACT	c. THIS PAGE			
unclassified	**unclassified**	**unclassified**	**UU**	**6**	

corresponding to the solution of the wave equation is given by:

$$f_n = \frac{n}{2L}\sqrt{\frac{T}{m_c}},$$

where T is cable tension, m_c is mass per unit length of the cable, and L is the cable length. Figure 1 depicts notionally the interaction of the Strouhal excitation with the structural modes of the array. Cable strum due to vortex shedding is strongly excited when the Strouhal excitation frequency is closely aligned with a resonant mode of the cable transfer function.

2.2 Wavenumber-frequency analysis

The decomposition of an array snapshot into its constituent acoustic and non-acoustic components is accomplished using a wavenumber-frequency, or k-ω, transform. The k-ω transform is a 2-d FFT in space and time. Maximum unambiguous wavenumber resolvable is equal to π/d, where d is the sensor spacing. Resolution in wavenumber is governed by the aperture length, L. For non-dispersive propagation, frequency and wavenumber are linearly related via

$$k(f) = \frac{2\pi f}{c_p},$$

where c_p equals the phase speed of the wavefront.

Figures 2 and 3 depict k-ω plots for two towed arrays under consideration in this work. The first exhibits superior vibration isolation and higher resolution due to its longer aperture. This array experiences only weak sidelobe leakage of vibrational modes into the acoustic cone. As such, under nominal operating conditions, this array does not exhibit a pronounced cable strum interference problem. The second array is characterized by limited vibration isolation. It is subject to significant leakage of vibrational energy into the acoustic cone via mainlobe penetration in forward endfire. Leakage of vibrational energy into acoustic forward endfire is a strong function of own-ship tow speed. For this array, which is the subject array for this paper, cable strum represents a significant mainlobe interference problem.

3. BEAMSPACE ABF FOR CABLE STRUM

The ABF architecture under consideration in this paper consists of a frequency-domain beamspace adaptive beamformer. The adaptive beamspace consists of a 7-dimensional beam fan with fixed cosine spacing. The beam fan translates with steering direction.

The beamspace ABF derives its cable strum nulling capability from the fact that near endfire the beam fan is partially composed of beams steered to high wavenumber non-acoustic space.

For each time epoch, the element timeseries are transformed to the frequency domain via FFT. A beamspace covariance matrix is formed for each frequency bin independently and a 7-dimensional beamspace MVDR weight vector is subsequently computed. Adaptation control is governed by setting a limit on the maximum allowable white noise gain for the adaptive processor.

3.1 White Noise Gain

White noise gain (WNG) is defined as the gain applied by the adaptive beamformer to a spatially white input noise process, and is represented by

$$\mathbf{WNG} = \overline{w}^H \overline{w},$$

where $\boldsymbol{w}$ represents the MVDR beamformer steering vector given by

$$\overline{w} = \frac{R^{-1}\overline{v}}{\overline{v}^H R^{-1}\overline{v}}.$$

The vector $\boldsymbol{v}$ represents the CBF weight vector and the matrix $\boldsymbol{R}$ denotes the sample covariance for the current processing bin. (Actually, the beamformer WNG is a quantity equally applicable to the output of the CBF beamformer, expressed as $\boldsymbol{v}^{\mathbf{H}}\boldsymbol{v}$). Beamformer WNG is a measure of the level of mainlobe adaptive nulling effected by the beamformer steering vector. As such, a constraint on maximum allowable WNG can be used to control the level of mainlobe adaptation of the adaptive beamformer relative to that of the ideal conventional beamformer:

$$\overline{w}^H \overline{w} \le \frac{\beta}{N}.$$

Here β is a constant ranging from 1 to infinity, with 1 representing CBF performance (no adaptive nulling capability and best robustness to mismatch) and infinity representing MVDR performance (most adaptive nulling capability and most sensitivity to mismatch). Note that under this convention, the quantity $\boldsymbol{1/N}$ represents the WNG of the conventional CBF beamformer, where N equals the number of elements in the array.

The relative WNG is a particularly important metric to consider when the source of interference lies within the beamformer mainbeam. Figure 4 depicts the behavior of the WNG of the minimum variance distortionless

response (MVDR) ABF relative to that of CBF for a simulation scenario in which an interferer is swept across cosine space and permitted to penetrate the beamformer mainbeam. An elevation in WNG results from the ABF algorithm attempting to drive a mainlobe null concurrent with satisfying the MVDR unity gain constraint in the steering direction. The three inset figures show ABF (shown in red) and CBF (shown in blue) beampatterns in the vicinity of the steering direction for three different interferer cosine positions. The sequence attempts to connect the WNG cosine dependence with the ABF beampattern shape as the interferer cosine approaches the steering direction. When the interferer is far in the sidelobe of the array beampattern (inset 3), the ABF and CBF mainlobe beampatterns effectively overlap. In this case, a simple sidelobe null (not pictured) is all that is needed in order to maximize signal-to-interference-plus-noise ratio (SINR). As the interferer penetrates the mainbeam, a squinting or splitting of the adaptive beampattern occurs coincident with the introduction of a mainlobe null. This squinting is the result of the beamformer's attempt to maximize SINR by trading off interference suppression against excess white noise gain in the vicinity of the steering direction.

3.2 Adaptivity/Robustness Tradeoff

Figure 4 illustrated how an elevation in WNG occurs in response to a mainlobe interferer. We may conclude that WNG is a measure of the mainbeam adaptive nulling being performed by the ABF. It is important to understand that the ABF algorithm is unable to distinguish between most forms of signal model mismatch and a mainlobe interferer. Thus, the ABF will interpret steering vector mismatch as mainlobe interference and attempt to cancel it as well. Some degree of steering vector mismatch is unavoidable in real towed array data applications. Common sources of mismatch include manifold uncertainty, sensor calibration error, and unmodeled multipath propagation. The beamformer signal model is based on an assumption of a perfect plane wave with known sensor gain and known relative sensor location. As the ABF algorithm will attempt to null any data component that deviates from these assumptions, self-nulling due to steering vector mismatch is a major concern. By imposing a constraint on the maximum allowable WNG of the adaptive beamformer, robustness to mismatch induced nulling may be introduced.

Analyses of towed array data have shown that to effect a useful level of strum rejection using the beamspace ABF algorithm, a fairly aggressive adaptation strategy is required. By contrast, signal protection against self-nulling in the cable strum band requires a very conservative adaptation approach. In this work, it was empirically determined that a WNGC of 6 dB, or a maximum allowable WNG of 4x that of the CBF beamformer, represents the best compromise between mainlobe cable strum nulling and signal preservation in the presence of mismatch.

3.3 Adaptive Weight Power Scaling

The white noise gain constraint (WNGC) employed in the beamspace ABF architecture is based on the scaled projection technique first proposed by Cox *et al.* [4].

The scaled projection WNGC implementation is composed of two essential parts. First, the MVDR weight vector is decomposed into two orthogonal components, non-adaptive and adaptive components respectively, using the following beamspace projection operators:

$$\boldsymbol{P}_{na} = \frac{\bar{v}\bar{v}^{H}}{\bar{v}^{H}\bar{v}}, \quad \boldsymbol{P}_{a} = \boldsymbol{I} - \boldsymbol{P}_{na}$$

Second, upon a WNG threshold exceedance, the adaptive component thus isolated is scaled such that the WNGC at the beamformer output is met exactly.

The orthogonal decomposition prior to adaptive weight scaling is important. This step guarantees that the weight scaling will be applied only to the adaptive, or data-dependent, component of the ABF weight vector. This insures that the scaling process does not modify, scale, or rotate the beamformer response to a signal that is perfectly matched to the steering vector. Consequently, the scaling preserves the constraint of distortionless response in the steering direction. The adaptive component of the MVDR weight vector is given by:

$$\bar{w}_{a} = \boldsymbol{P}_{a}\bar{w}.$$

It is straightforward to verify that the non-adaptive and adaptive components derived in this way are indeed orthogonal. The scaled output weight vector is then given by:

$$\bar{w}_{o} = \bar{w}_{na} + k\bar{w}_{a},$$

where the scalar, k, represents the scaling coefficient. We then specifiy the WNGC at the output of the beamspace ABF processor in terms of a multiplier on the non-adaptive WNG,

$$\bar{w}_{o}^{H}\boldsymbol{T}^{H}\boldsymbol{T}\bar{w}_{o} \le \alpha\ \bar{w}_{na}^{H}\boldsymbol{T}^{H}\boldsymbol{T}\bar{w}_{na}.$$

Here, $\boldsymbol{T}$ represents the 7-dimensional transformation from element space to adaptive beamspace. For a 6 dB WNGC the multiplier, α, is equal to 4. Solving the constraint equation results in a quadratic on the scaling coefficient, k [5]. The result is two solutions for k which meet the constraint exactly. We choose the value which minimizes the output power of the ABF. This procedure is carried out at each processing epoch and for each frequency bin

independently. A geometric interpretation of the weight scaling procedure is shown in Figure 5.

4. TOWED ARRAY DATA RESULTS

Figure 6 depicts frequency-azimuth (FRAZ) plots for a typical time epoch for each of four different processors: a) the CBF beamformer, 2) the conservative baseline ABF beamformer, 3) the aggressive 6 dB WNGC ABF optimized for strum rejection, and 4) unconstrained MVDR. The baseline ABF represents the WNGC as implemented in the present towed array processing system. While the details of this WNGC implementation are not presented here, the basic design philosophy of this ABF algorithm is to emphasize robustness to mismatch effects. Upon exceeding the WNG threshold, set in the vicinity of 2 dB, the baseline ABF scales the adaptive weight vector back to the non-adaptive or CBF weight vector. This severely constrains the ability of the baseline ABF to effectively null any strong mainlobe interference such as cable strum.

In Figure 6, the presence of a strong interference source with multiple sidelobes is observed near broadside in the CBF FRAZ display. As expected all of the ABF approaches, conservative and aggressive alike, demonstrate the capacity to null such a strong discrete sidelobe interference source. This result thus serves as a useful consistency check of algorithm implementation.

Next, we direct our attention to the cable strum interference near forward sector, i.e. near cosine equal to 1. In the normalized frequency band f = 0-0.3, cable strum is observed to extend over a wide sector of cosine space from forward endfire to near broadside. The important differences between the conservative and aggressive ABF approaches are apparent from the cable strum rejection performance in this frequency band. The conservative ABF algorithm does very little to reduce the amplitude of the strum interference in forward endfire. The bearing extent of the strum is reduced slightly. With its 6 dB WNGC, the bearing extent and amplitude of the cable strum is significantly curtailed relative to that of the conservative baseline ABF algorithm.

Figure 7 shows raw power spectrum density plots to further illustrate the performance improvement realized with increasingly aggressive adaptation. Notice that the cable strum ABF achieves as much as a 15 dB local suppression of the strum-dominated noise floor in the normalized frequency band f = 0.1-0.3. The resulting noise floor suppression uncovers the presence of a narrowband feature at f = 0.2 that was otherwise undetectable in the CBF and baseline ABF configurations.

Figure 8 shows the measured WNG plots corresponding to the power spectrum density plots of Figure 7. The measured WNG illustrates the relationship between WNGC and strum rejection. It is clear that at a WNGC of 6 dB most of the strum noise floor suppression performance is realized. Recall that the point here is to allow the ABF algorithm to adapt only as much as necessary to effect useful cable strum noise suppression.

5. CONCLUSIONS

Mechanically induced towed array self-noise limits detection performance in passive sonar systems, particularly at forward endfire. In this work, a beamspace adaptive beamforming architecture for the rejection of strong mainlobe cable strum rejection in forward endfire was presented. The approach focused on the choice of a white noise gain constraint which achieved a suitable balance between aggressive adapation for effective strum nulling and conservative adaptation for robustness to mismatch-induced self-nulling. A WNGC of 6 dB relative to the WNG for the non-adaptive steering vector was empirically determined to offer the best balance. The WNGC implementation was based on the scaled projection technique first presented by Cox et al. [4]. Significant cable strum suppression performance was shown to be possible, on the order of 15 dB locally within the strum interference band.

6. REFERENCES

[1] J. W. Bedenbender, R. C. Johnston, and E. B. Neitzel, “Electroacoustic characteristics of marine seismic seismic streamers,” *Geophysics*, vol. 35, no. 6, Dec. 1970, pp. 1054-1072.

[2] V. Premus, ``Adaptive Self-Noise Suppression for Passive Sonar Towed Arrays,” *Proceedings of the Eighth Annual Workshop on Adaptive Sensor Array Processing, ASAP 2000*, MIT Lincoln Laboratory, March, 2000.

[3] L. Prandtl, “The generation of vortices in fluids of small viscosity,” *J. Royal Aeronautical Society,* Vol. 31, Dec. 1927, pp. 720-741.

[4] H. Cox, R. Zeskind, and M. Owen, ``Robust Adaptive Beamforming,” *IEEE Trans. on ASSP*, Vol. 35, No. 10, Oct., 1987.

[5] Z. Tian, K. Bell, and H. Van Trees, ``A Recursive Least Squares Implementation for Adaptive Beamforming Under Quadratic Constraint,” *IEEE Trans. on SP*, Feb. 2000.

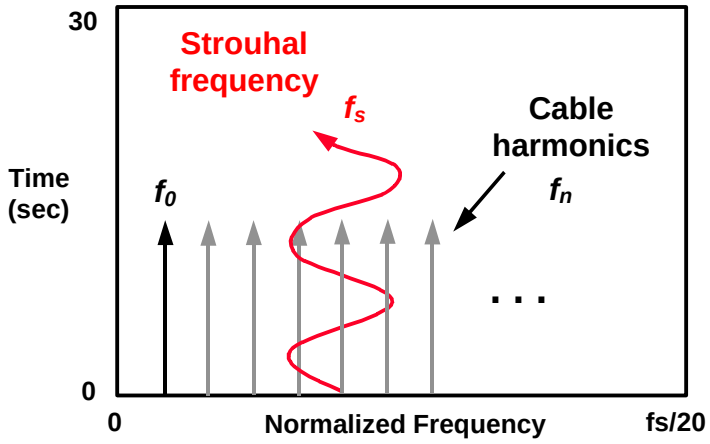

Figure 1: Notional depiction of time varying Strouhal excitation and array vibrational modes.

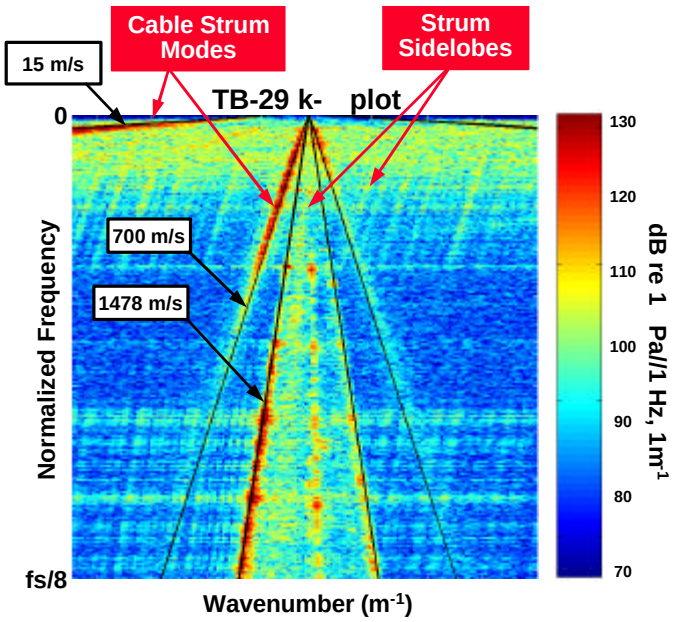

Figure 2: Frequency-wavenumber plot for TB-29 array.

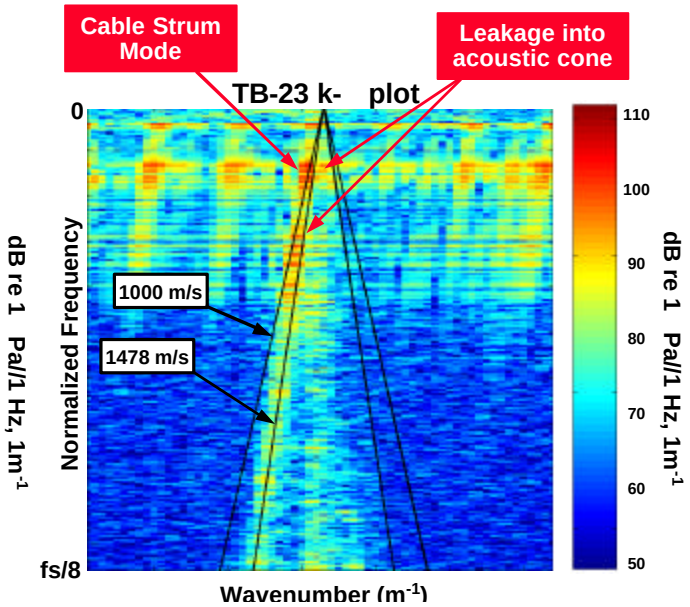

Figure 3: Frequency-wavenumber plot for TB-23 array.

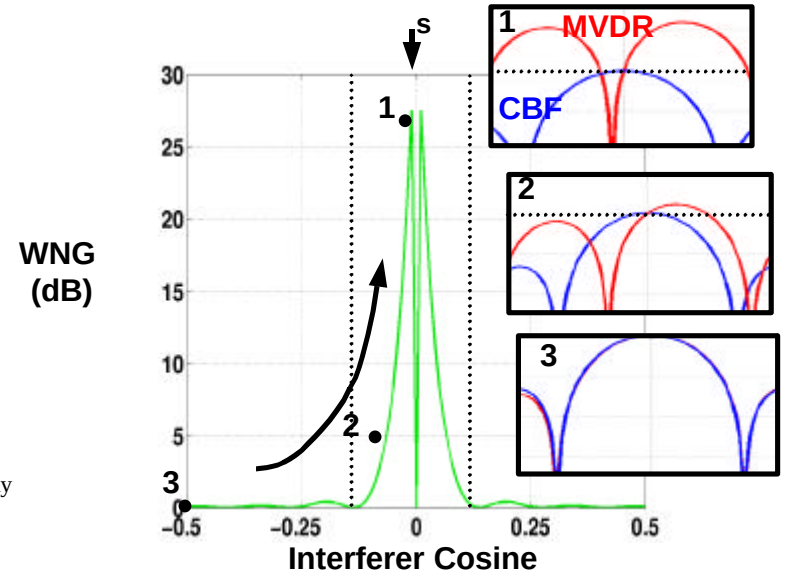

Figure 4: Simulated white noise gain plot and associated CBF and MVDR beampatterns.

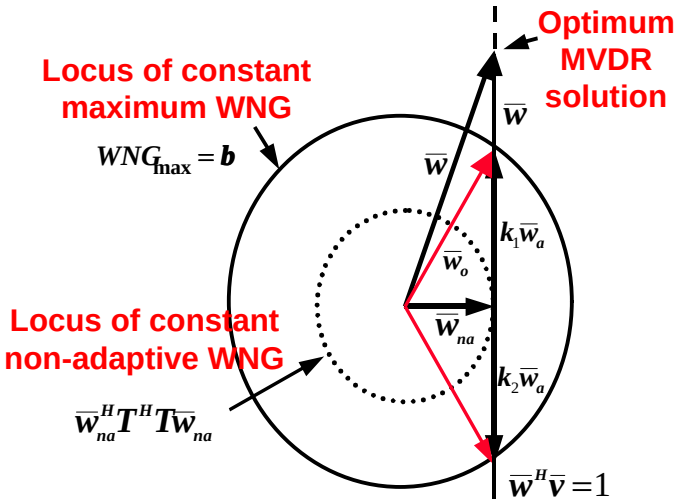

Figure 5: Geometric interpretation of scaled projection weight scaling technique.

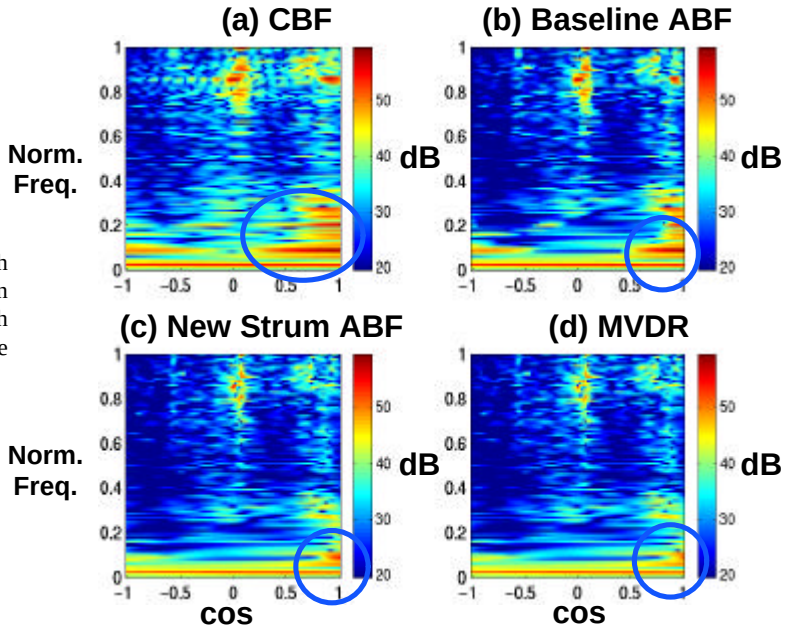

Figure 6: Frequency-Azimuth plots depicting reduction in cable strum cosine extent with increasingly more aggressive adaptation.

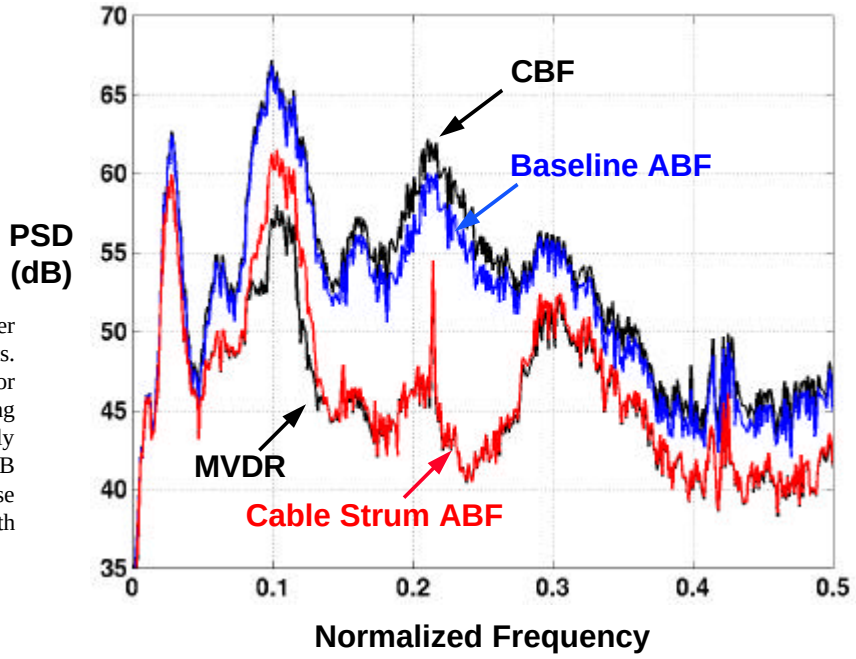

Figure 7: Raw power spectrum density plots. illustrating strum noise floor suppression with increasing levels of adaptation. Locally as much as 15 dB improvement in strum noise suppression is realized with 6 dB WNGC.

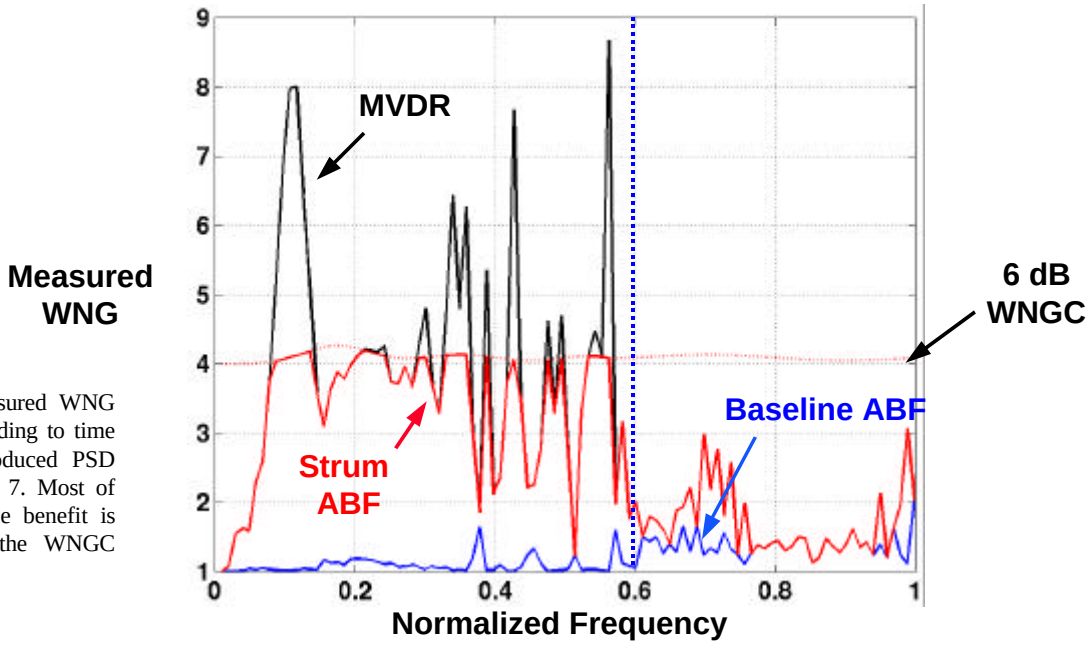

Figure 8: Measured WNG plots corresponding to time epoch that produced PSD plots in Figure 7. Most of the performance benefit is realized with the WNGC equal to 6 dB.